

**Brazilian Journal of
Chemical Engineering**

**Numerical investigation of gas-solid flow behavior in a
novel integral multi-jet spout-fluidized bed**

| | |
|-------------------------------|--|
| Journal: | <i>Brazilian Journal of Chemical Engineering</i> |
| Manuscript ID | BJCE-2018-0139 |
| Manuscript Type: | Original Article |
| Date Submitted by the Author: | 11-Apr-2018 |
| Complete List of Authors: | Wu, Feng; School of Chemical Engineering, School of Chemical Engineering Zhang, Xuan; School of Chemical Engineering, Northwest University Zhou, Wen; School of Chemical Engineering, Northwest University Ma, Xiao; 1514276826 |
| Keyword: | Integral multi-jet spout-fluidized bed, Gas-solid flow behavior, CFD, Enhancement of particle radial motion, Coefficient of variation |
| | |

SCHOLARONE™
Manuscripts

1
2
3 Numerical investigation of gas-solid flow behavior in a novel integral
4 multi-jet spout-fluidized bed
5
6
7
8
9

10 Feng Wu^{1*}, Xuan Zhang¹, Wenjing Zhou², Xiaoxun Ma¹
11
12 1, School of Chemical Engineering, Northwest University, Xi'an, China
13 2, School of Chemical Engineering and Technology, Xi'an Jiaotong University, Xi'an, China
14
15 *Corresponding author:
16 Email: wufeng@nwu.edu.cn
17 Tel: +86-15309202861
18
19
20
21
22 **Abstract:** The gas-solid flow behavior in a novel integral multi-jet spout-fluidized bed (IMJSFB) was
23 numerically simulated using Eulerian-Eulerian two-fluid model (TFM) including the kinetic theory of granular flows. A
24 number of slits (4) were formed on cone side of the cylindrical spouted bed to form auxiliary multi-jet structure, which
25 can create spoiler effects on the boundary of the pyramidal. The distributions of particle velocity and concentration in the
26 IMJSFB were obtained by numerical simulation, which were compared with simulation results of a single nozzle spouted
27 bed. The CFD results show that compared with the conventional spouted beds, the IMJSFB structure can effectively
28 enhance the particle's velocity in annulus of spouted bed (especially in destroying flow dead zone at the annulus). The
29 enhanced particle motion significantly decreases the volume fraction of the boundary layer on the cone. The particle
30 concentration and velocity distribution along the radial direction becomes more uniform, and the decrease in value of
31 coefficient of variation (CV) of particles' velocity is 22.9% in IMJSFB. Also, the turbulent kinetic energy of gas phase
32 can be significantly enhanced by fluidizing gas and the strengthening effect on turbulent kinetic energy of gas keeps
33 good with the increase of the bed height.
34
35
36
37
38
39
40
41
42
43
44
45
46
47
48
49
50
51
52
53
54
55
56
57
58
59
60

Key words: Integral multi-jet spout-fluidized bed; Gas-solid flow behavior; CFD; Enhancement of particle
radial motion; Coefficient of variation

1 2 3 1. Introduction

4 Spouted beds are gas-particle contactors which provide a means of good mixing and circulation for particles of
5 relatively large size and wide size distribution. The spouted bed technique has been widely used in petro-chemical,
6 chemical, nuclear engineering and metallurgical industries (Epstein et al., 2011; Ichikawa et al., 2003), such as drying of
7 granular material, granulation, black liquor, polymerizations, pyrolysis, gasification and nuclear fuel coating because of
8 their efficiency in providing effective gas-coarse particle contact. In the past, many experimental and numerical studies
9 have been performed to better understand the behavior of spouted beds. Ichikawa et al. (2003) described particulate
10 design and preparation to control drug release thermosensitively or in a delayed mode from microcapsules (MCs) that
11 were prepared by coating with a membrane incorporating hydrogel as a particulate or chemical component and the
12 particulate preparation was carried out by a spouted bed coating process. Freitas et al. (1997) experimentally studied
13 the dynamics of a spouted bed with particle feed through the base. They compared two methods of measuring the
14 superficial air velocity in the annular region, and analyzed the effects of the particle feed rate, air flow rate and bed
15 height on the spouted bed dynamics. Olazar et al. (2002) have experimentally tested the feasibility of the thermal
16 processing at low temperature of straw black liquor in fluidized and spouted bed. Experiments in different operating
17 conditions were carried out in order to get a basic knowledge about the behavior of this residue during pyrolysis,
18 gasification, and combustion processes. Niksiar et al. (2014) have adopted the streamtube modeling technique with a
19 new approach and a hydrodynamic model in conical spouted beds, and none of the required empirical equations in the
20 well-known streamtube model are needed to predict hydrodynamic parameters. Xavier et al. (2016) experimentally
21 investigated the fluid dynamics of a mixture of sand and macadamia shell in a conical spouted bed, with different mass
22 fractions and static bed heights. The particles exhibited good circulation in the bed for mass fractions of 25% to 75%,
23 with acceptable levels of segregation for pyrolysis process. Parise et al. (2017) experimentally studied hydrodynamics of
24 a slot-rectangular spouted bed of biomass particles with simultaneous injection of spouting and pulsating air streams.
25 They found that, at constant average pulsation gas volumetric flow rate and bed depth, a pulsation frequency of 5 Hz
26 required the least total air flow to achieve spouting. However, for low pulsation volumetric flow rate, the effect of the
27 pulsation frequency became less evident for deep beds than for shallow ones. Kiani et al. (2017) experimentally
28 investigated the mixing and segregation of binary mixtures of particles with different sizes and densities in a pseudo-2D
29 spouted bed. They found that the segregation of solid particles and the time to equilibrium both decreased when the
30 air velocity increased to a magnitude much larger than the minimum spouting velocity, and the axial segregation
31

1
2
3 increased with the diameter ratio of the particles. Szafran et al. (2004) have built CFD modeling of heat and mass
4 transfer in a spouted bed dryer with a draft tube. A heat- and mass-transfer model was added as compiled executable
5 code by means of UDF programming to FLUENT 6.1. Liu et al. (2012) numerically simulated the UO₂ kernel coating
6 process of spouted bed dynamics in the coater. They found that the maximum spouted height could be mainly
7 determined by the gas velocity if the packing heights of particles were the same. Recently, Hosseini et al. (2017)
8 numerically investigated effects of the presence of draft plates on the hydrodynamics and heat transfer behavior of solid
9 particles in the spouted beds. Wu et al. (2018) compared mixing behaviors of gas and particle phases in three types of
10 spouted beds: without disturbance units, with a pair of balls and with a pair of longitudinal vortex generators (LVGs).
11 They found that the radial velocity and granular temperature of particle phase in spouted bed can be promoted
12 significantly by longitudinal vortex.
13
14

15 In order to improve gas-solid flow in the spouted or fluidized beds, reduce the dead zone at the bottom of the
16 annulus and allow for easier particle clustering in the annulus regions, the fluidized gas is introduced through a
17 perforated distributor surrounding the central nozzle. Sutanto et al. (1985) experimentally investigated a half-column
18 spouted bed incorporating auxiliary flow. They identified and mapped four different flow regimes — fixed bed, spouting
19 with aeration, spout-fluidization and jet in a fluidized bed, they also found that solids circulation was increased
20 somewhat by addition of auxiliary flow for deep beds, but a decrease occurred for shallow beds. Zhao et al. (1987)
21 revealed that the addition of auxiliary air along the conical base of a spouted-fluid bed leads to more uniform axial
22 temperature profiles. Apnold et al. (1992) introduced an air-blown spouted fluidized bed gasification process for the
23 production of low calorific value fuel gas by British Coal Corporation. Pianarosa et al. (2000) experimentally studied
24 gas-solid flow in a cylindrical spout-fluid bed. They found that auxiliary air led to some decrease in particle velocities in
25 the spout and to a modest decrease in the net solids circulation rate. Zhong et al. (2005,2005a,2005b) obtained
26 differential pressure fluctuation time series at different locations in a two-dimensional spout-fluid bed with a cross
27 section of 300 × 30 mm and height 2000 mm, they examined the effects of two important operating parameters
28 (spouting gas velocity and fluidizing gas flow rate) on the Shannon entropy, and proposed some suggestions for the
29 operation of spout-fluid bed coal gasifiers. They also established a two-dimensional cold model of a spout–fluid bed coal
30 gasifier with its cross section of and height of 2000 mm to investigate the jet penetration depth. Wang et al. (2014)
31 numerically simulated the flow behavior of gas–solid phases using the Eulerian–Eulerian two-fluid model (TFM)
32 approach with kinetic theory for granular flow to obtain the flow patterns in spouted-fluid beds. They found that the gas
33

1
2
3 flux and gas incident angle have a significant influence on the porosity and particle concentration in gas-solid
4 spouted-fluid beds, and the fluidizing gas flux affects the flow behavior of particles in the fountain. Nagashima et al.
5 (2015) experimentally studied and compared the effects of operating parameters on flow characteristics of the
6 spout-fluid bed (SFB) and the SFB with a draft tube in the bed (DSFB) using the same semi-cylindrical column and the
7 same particles. They found that the flow regime maps were recognized based on pressure fluctuation data and the
8 DSFB had a wide range of operating conditions for stable spouting, comparing with the SFB. Sutkar et al. (2016)
9 presented a novel CFD - DEM model for coupled heat and mass transfer in a spout fluidized bed with liquid injection.
10 They performed a number of tests to determine the optimum particle collision time step by analysing the error in the
11 prescribed restitution coefficient (difference between defined and applied values). Monazam et al. (2017,2017a)
12 experimentally investigated the pressure drop and its associated superficial gas velocity in a flat based spouted bed
13 operating with and without fluidization. In addition, they experimentally studied characteristics of a cylindrical
14 spout-fluidized bed (I.D.=10 cm) with different static heights and two materials (Al_2O_3 and high density polyethylene).
15 They compared the results of minimum spouting velocity obtained in their study with reported correlations for both
16 spouted and spout-fluidized beds, and considerable discrepancies were found among the values obtained using
17 different model equations, also when compared to experimental results.

18
19
20
21
22
23
24
25
26
27
28
29
30
31
32 The present review of literature shows that an investigation on the gas-solid flow behavior in the spouted-fluid beds
33 with auxiliary gas from the conical base using Eulerian–Eulerian two-fluid model (TFM) is still required. Moreover, the
34 existing multi-jet spouted-fluidized bed needs bypass to maintain the lateral air flux, which increases the bypass
35 equipment. In order to overcome this shortcoming, a novel integral multi-jet spout-fluidized bed (IMJSB) is designed to
36 improve gas-solid flow in the spouted bed and reduce the dead zone at the bottom of the annulus while the bypass air
37 supplied by auxiliary equipment is omitted.

38
39
40
41
42
43
44 Thus, the main objective of the present paper is to study the improvement of gas-solid radial mixing in the integral
45
46 multi-jet spout-fluidized bed without air supplied auxiliary equipment. ~~The Gidaspow drag model (Gidaspow et al., 1992a)~~
47
48 is chosen to describe the interface momentum exchange, and the two-fluid model (TFM) is used. In the following
49 sections, firstly, the physical models and mathematical formulations of the problem are given. Subsequently, the
50 gas-solid two-phase flow behavior in a single nozzle spouted bed (SNSB) and an integral multi-jet spout-fluidized bed
51
52 (IMJSFB) were compared and analyzed in detail. Finally, the conclusions are given.

1

2

3 2. CFD model for spouted beds

4 2.1. Gas-solid two-fluid model

5 The governing equations and the associated constitutive models of the Eulerian-Eulerian TFM that are used in the
 6 simulation of single nozzle spouted bed and integral multi-jet spouted bed are summarized in this section. Using the
 7 kinetic theory of granular flows (Ding et al., 1990), the viscous forces and the pressure of solids phase can be described
 8 as a function of the granular temperature (Lun et al., 1984). The stress of solids phase due to frictional interactions
 9 between particles is represented by the Schaeffer model (Schaeffer et al., 1987) and the diffusion coefficient of granular
 10 energy by Gidaspow model (Du et al., 2006) is used. The governing equations and constitutive relations for spouted
 11 beds are shown in Table 1.

12

13 In this work, three kinds of turbulence models (Standard k- ε model (Lauder et al., 1974), RNG k- ε model (Yakhot
 14 et al., 1986), Realized k- ε model (Shih et al., 1995)) were adopted when studying the hydrodynamics of gas and particles
 15 in cold spouted bed at constant ambient temperature, and compared with the experimental data (Figure 3). It can be
 16 seen from figure 3 that the differences between simulation results made by three different turbulence models are very
 17 small. As a result, the standard k- ε turbulence model is adopted in the simulations of this paper and the dispersed
 18 turbulence model has been adopted, where turbulence predictions for gas phase are obtained by the standard k- ε
 19 model supplemented with extra terms that include the inter-phase turbulent momentum transfer. The equations of k- ε
 20 turbulence model are shown in Table 1 by $\mu_t = C_\mu \rho_g k^2 / \varepsilon$, where the equations of turbulent kinetic energy and turbulent
 21 kinetic energy dissipation rate are expressed by Eqs.(T1-7) and (T1-8). The empirical constants, C_1 , C_2 , C_μ , σ_k , and σ_ε
 22 are 1.44, 1.92, 0.09, 1.0 and 1.3, respectively. In order to couple the momentum transfer between gas and particle phase,
 23 a model for the drag force is required. Du et al. (2006) investigated the influence of different drag models on the
 24 hydrodynamics of spouted bed, and concluded that the Gidaspow drag model (Gidaspow et al., 1992a) gave the best
 25 agreement with experimental data. Hence, the Gidaspow model has been adopted, and its expressions are also given in
 26 Table 1.

27

28

29

30

31

32

33

34

35

36

37

38

39

40

41

42

43

44

45

46

47

48

49

50 Table 1 Mathematical model of gas-solid flow in spouted beds

51

52

53

54

55

56

57

58

59

60

A. Conservation equations

(1) Continuity equations

(a) Fluid phase

$$\frac{\partial}{\partial t} (\alpha_g \rho_g) + \nabla \cdot (\alpha_g \rho_g v_g) = 0 \quad (T1-1)$$

(b) Solids phase

* Results in Fig.3 only indicates that simulations ~~results~~ results do not match w experiments.

$$\frac{\partial}{\partial t}(\alpha_s \rho_s v_s) + \nabla \cdot (\alpha_s \rho_s v_s v_s) = 0$$

v_s & v_g are missing in the
 λ, σ and μ in the list.

(T1-2)

(2) Momentum equations

(a) Fluid phase

$$\frac{\partial}{\partial t}(\alpha_g \rho_g v_g) + \nabla \cdot (\alpha_g \rho_g v_g v_g) = -\alpha_g \nabla P_g + \alpha_g \rho_g g + \beta_{gs} (v_s - v_g) + \nabla \cdot \tau_g \quad / \quad (T1-3)$$

(b) Solids phase

$$\frac{\partial}{\partial t}(\alpha_s \rho_s v_s) + \nabla \cdot (\alpha_s \rho_s v_s v_s) = -\alpha_s \nabla P_g + \nabla \cdot \tau_s + \alpha_s \rho_s g + \beta_{gs} (v_g - v_s) \quad / \quad (T1-4)$$

(3) Granular temperature equation (Ding et al., 1990)

$$\frac{3}{2} \left[\frac{\partial}{\partial t}(\alpha_s \rho_s \theta) + \nabla \cdot (\alpha_s \rho_s \theta) v_s \right] I = \left(-\nabla p_s I + \tau_s \right) : \nabla v_s + \nabla \cdot (k_s \nabla \theta) - \gamma_{\theta s} - 3\beta_{gs} \theta_s \quad / \quad (T1-5)$$

B. Constitutive equations

(a) Solids and gas phase stress tensors

$$\bar{\tau}_g = \alpha_g \mu_g \left[(\nabla v_g + \nabla v_g^T) - \frac{2}{3} \nabla v_g \bar{I} \right] \quad / \quad (T1-6)$$

$$\bar{\tau}_s = \alpha_s \mu_s \left[(\nabla v_s + \nabla v_s^T) + \alpha_s (\lambda_s - \frac{2}{3} \mu_s) \nabla v_s \bar{I} \right]$$

(b) Turbulent kinetic energy equation

$$\frac{\partial \alpha_g \rho_g k}{\partial t} + \nabla \cdot (\alpha_g \rho_g v_g k) = \nabla \left(\alpha_g \frac{\mu_t}{\sigma_k} \nabla k \right) + \alpha_g G_k - \alpha_g \rho_g \varepsilon \quad / \quad (T1-7)$$

(c) Turbulent kinetic energy dissipation rate equation

$$\frac{\partial \alpha_g \rho_g \varepsilon}{\partial t} + \nabla \cdot (\alpha_g \rho_g v_g \varepsilon) = \nabla \left(\frac{\mu_t}{\sigma_k} \nabla \varepsilon \right) + \alpha_g \frac{\varepsilon}{k} [C_1 G_k - C_2 \rho_g \varepsilon] \quad / \quad (T1-8)$$

$$G_k = \mu_t \left(\nabla v_g + (\nabla v_g)^T \right) : \nabla v_g$$

(d) Solids phase stress

$$\tau_s = \xi_s (\nabla \cdot v_s) I + \mu_s \left[[\nabla v_s + (\nabla v_s)^T] - \frac{1}{3} (\nabla \cdot v_s) I \right] \quad / \quad (T1-9)$$

(e) Solids pressure

$$p_s = \alpha_s \rho_s \theta + 2 \rho_s (1 + e_s) \alpha_s^2 g_0 \theta \quad / \quad (T1-10)$$

(f) Shear viscosity of solids (Du et al., 2006)

$$\mu_s = \phi_l(\alpha_s) \mu_{s,k} + (1 - \phi_l(\alpha_s)) (\mu_{s,k} + \mu_{s,f}) \quad / \quad (T1-11)$$

$$\mu_{s,k} = \frac{4}{5} \alpha_s^2 \rho_s d g_0 (1 + e) \sqrt{\frac{\theta}{\pi}} + \frac{10 \rho_s d \sqrt{\pi \theta}}{96 (1 + e) \alpha_s g_0} \left[1 + \frac{4}{5} \alpha_s g_0 (1 + e) \right]^2 \quad / \quad (T1-12)$$

$$\mu_{s,f} = p_{s,f} \sin(\psi) / 2 \sqrt{I_{2D}} \quad / \quad (T1-13)$$

(g) Bulk solids viscosity (Lun et al., 1984)

$$\xi_s = \frac{4}{3} \alpha_s^2 \rho_s d g_0 (1 + e) \sqrt{\theta / \pi} \quad / \quad (T1-14)$$

(h) Frictional viscosity (Schaeffer et al., 1987)

$$\mu_{s,fr} = \frac{P_s \sin \phi}{2 \sqrt{I_{2D}}} \quad / \quad (T1-15)$$

(h) Collisional energy dissipation (Lun et al., 1984)

$$\gamma_s = \frac{12(1 - e_s^2) g_0}{d_s \sqrt{\pi}} \rho_s \alpha_s^2 \theta_s^{3/2} \quad / \quad (T1-16)$$

(i) Radial distribution function at contact

$$g_0 = \left[1 - \left(\alpha_s / \alpha_{s,\max} \right)^{1/3} \right]^{-1} \quad (\text{T1-17})$$

(j) Diffusion coefficient of granular energy (Gidaspow et al., 1992a)

$$k_{\theta s} = \frac{150 d_s \rho_s \sqrt{\theta \pi}}{384(1+e_s) g_0} \left[1 + \frac{6}{5} \alpha_s g_0 (1+e_s) \right]^2 + 2 \rho_s d_s \alpha_s^2 g_0 (1+e_s) \sqrt{\frac{\theta}{\pi}} \quad (\text{T1-18})$$

(l) Interface momentum transfer coefficient (Gidaspow et al., 1992a)

$$\beta_{gs} = 150 \frac{\alpha_s^2 \mu_g}{\alpha_g d_s^2} + 1.75 \frac{\alpha_s \rho_g |u_g - u_s|}{d_s}, \quad \alpha_g < 0.8 \quad (\text{T1-19})$$

$$\beta_{gs} = \frac{3}{4} C_D \frac{\alpha_s \alpha_g \rho_g |u_g - u_s|}{d_s} \alpha_g^{-2.65}, \quad \alpha_g \geq 0.8 \quad (\text{T1-20})$$

$$C_D = \begin{cases} \frac{24}{\alpha_g \text{Re}_s} \left(1 + 0.15 (\alpha_g \text{Re}_s)^{0.687} \right), & (\text{Re}_s < 1000) \\ 0.44, & (\text{Re}_s \geq 1000) \end{cases} \quad (\text{T1-21})$$

$$\text{Re}_s = \frac{\rho_g d_s |u_g - u_s|}{\mu_g} \quad (\text{T1-22})$$

2.2. Simulation conditions

The experimental data of (He et al., 1994; He et al., 1994a) for cylindrical spouted bed with conical base are used to validate the conventional single nozzle spouted bed. The schematic of geometry, size and grids description of the IMJSFB are shown in Figure 1, and the corresponding parameters selected for the present simulation of single nozzle and multi-jet spouted bed are listed in Table 2. The boundary conditions for numerical simulation are listed in Table 3.

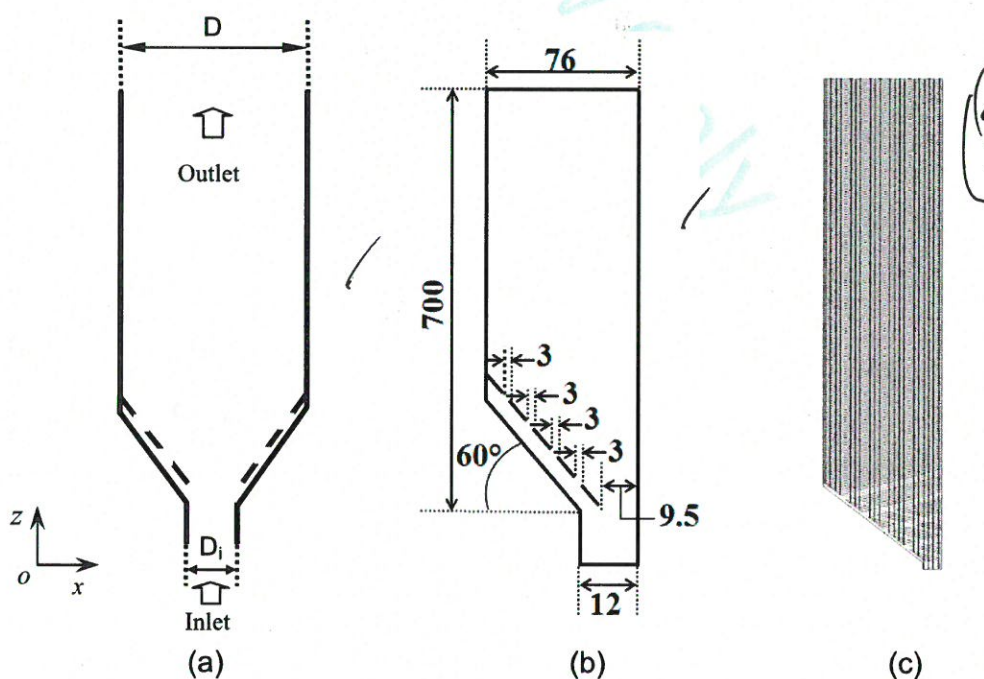


Fig.1 Schematic of (a) geometry, (b) size, and (c) grids of the IMJSFB (side jet number:4, unit: mm)

Table 2 Experimental and simulation data for two kinds of spouted beds

| Description | SNSB | IMJSFB |
|---------------------------------|-------------------------|-------------------------|
| Particle density | 2503 kg/m ³ | 2503 kg/m ³ |
| Gas density | 1.225 kg/m ³ | 1.225 kg/m ³ |
| Gas viscosity | 1.7894E-05 Pa·s | 1.7894E-05 Pa·s |
| Particle diameter | 1.41 mm | 1.41 mm |
| Maximum solid volume fraction | 0.59 | 0.59 |
| Static bed depth | 325 mm | 325 mm |
| Diameter of the bed | 152 mm | 152 mm |
| Diameter of the spout gas inlet | 19 mm | 24 mm |
| Gas superficial velocity | 0.54 m·s ⁻¹ | 0.54 m·s ⁻¹ |
| Side jet number | / | 4 |
| Width of the side jet | / | 3 mm |

Table 3 Boundary conditions for numerical simulation

| Initial and boundary conditions | Parameter |
|---------------------------------|--|
| Inlet | The turbulent velocity distribution, spouting inlet gas velocity U_i (m·s ⁻¹), turbulence kinetic intensity is $k=2\%$ No particles enter for solid phase |
| Outlet | Uniform velocity distribution for fluid phase No particle exits for solid phase |
| Wall | No slip for fluid phase Zero shear stress for solid phase |

why?

2.3. Numerical simulation method

The set of governing equations presented in Section 2.1 is solved by CFD code (Fluent 15), and the set of governing equations have been solved by finite control volume technique, the Phase Coupled SIMPLE algorithm, which is an extension of the SIMPLE algorithm for multiphase flow, has been used for the pressure-velocity coupling and correction. A second-order upwind discretization scheme is used for momentum, turbulence kinetic energy and turbulence dissipation rate equations, and a first-order upwind scheme is used only for the volume fraction term. Transient simulations are performed with a constant time step of 2×10^{-5} s with 30 iterations per time step. The convergence criterions for the solution are that all variable residuals such as velocity are less than 1×10^{-3} . Structured grid is used in the computational domain of single and multi-jet spout-fluidized bed. A grid independence test is performed for the single nozzle spouted bed. It is found that the grid number of 13260 is sufficiently fine to ensure a grid independent solution, see Figure 2. Therefore, for the computations of single nozzle spouted bed in the present study the number of grid is set as 14391, and the total numbers of grid cells is 14760 for the IMJSFB.

↳ 2 or 3-D?

<https://mc04.manuscriptcentral.com/bjce-scielo>

{ quads?
triangles?

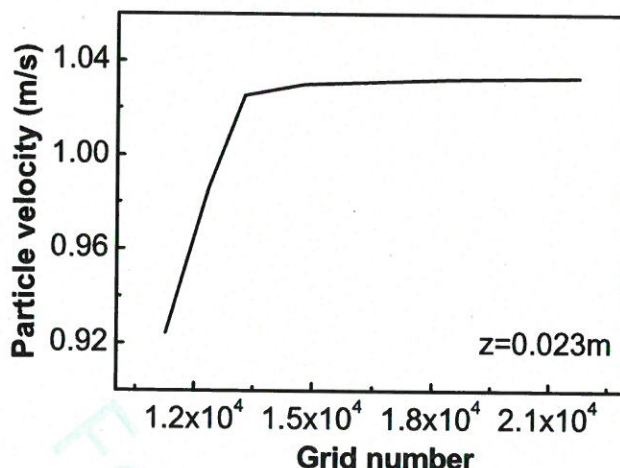
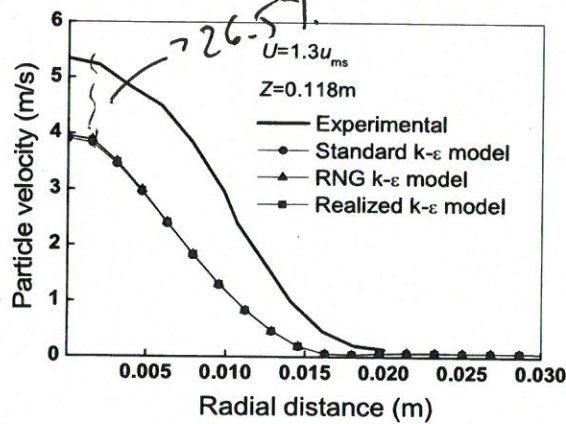
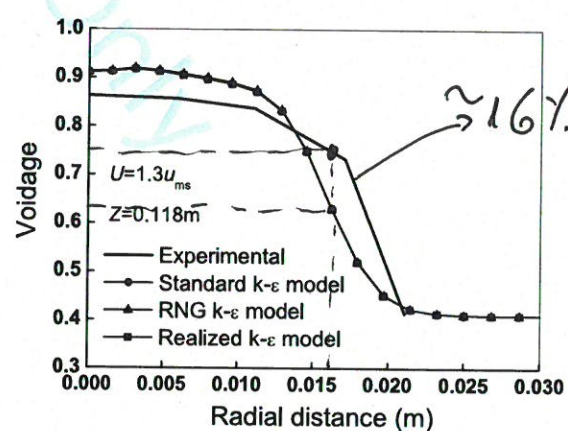


Fig. 2 Grid number independency test

To validate the computer code, problems on hydrodynamics in the conventional spouted (single nozzle spouted bed) were solved with three kinds of turbulence models and compared with the experimental profiles of the particle velocities (He et al., 1994; He et al., 1994a), as shown in Figure 3. The maximum deviations of particle velocity and voidage of gas phase at different heights in spouted bed are less than 26 % and 6.9 % between numerical results and experimental data, respectively. Considering the error produced by the measurement, we think that the deviation is acceptable, which can be attributed to the simulation of IMJSFB .



(a) Velocity of particle phase



(b) Voids of gas phase

Fig. 3 Comparison between numerical simulation results and experimental results of
Velocity of particle phase and voidage of gas phase in the SNSB

3. Results and discussion

3.1 Effect of integral multi-jet on particle concentrations

Figure 4 shows the comparison of particle concentrations in IMJSFB with an inlet gas nozzle velocity of 0.702 m/s in the stable state ($U=1.3U_{ms}, t=5$ s). It can be observed that when the spout time reached 5 seconds, the IMJSFB basically reached the steady state. The spouting gas with high velocity carries particles from the bottom to the top, and the fluidizing gas flowing out from auxiliary multi-jet acts as air jet with high velocity. As a result, the radial mixing of particles is intensified. More particles are carried into the spout and bubbles are formed because of the auxiliary air jets. Also, compared with the solid volume fractions in single nozzle spouted bed (Figure 5 (a)), a wave like spout structure without a fountain zone has been formed in IMJSFB because the additional bubbles emerge due to fluidizing gas and enter the spout zone and the area of spout region becomes wider in spouted bed.

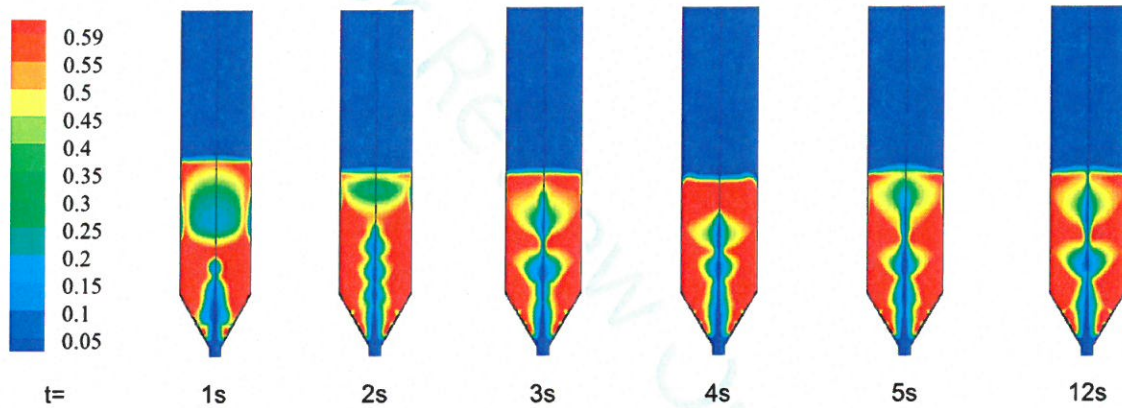


Fig. 4 Instantaneous concentration of particles in the IMJSFB with $U=1.3U_{ms}$

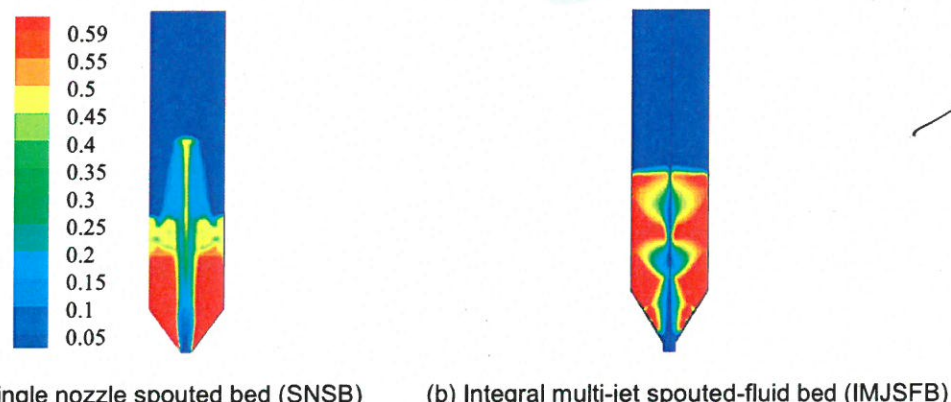


Fig. 5 Comparison of contour plots of solid volume fractions in two kinds of spouted beds

Figure 6 compares concentration of particles in two kinds of spouted beds at different spouted bed levels for $U=1.3U_{ms}$. Firstly, the particle volume fraction distribution in annulus region of IMJSFB is significantly lower than that of the single nozzle spouted bed, especially near the conical region ($z=0.023m$). It reveals that the auxiliary air jets set on side of the conical can effectively reduce the volume fraction of the annulus' particles, the particle volume fraction along the radial distribution becomes flat, which is beneficial to eliminate the "dead zone" of particle flow at the cone, thus improving the motion state of the particles and the gas-solid contact efficiency in the annular region, especially in the near cone region. As a result, the distributions of particles in the IMJSFB become more uniform. Secondly, it can be seen from Figure 6 that the concentration of particles in annulus of the IMJSFB increases with increasing of spouted bed levels, however, its overall radial distribution of particle concentrations are still lower than that of single nozzle spouted bed.

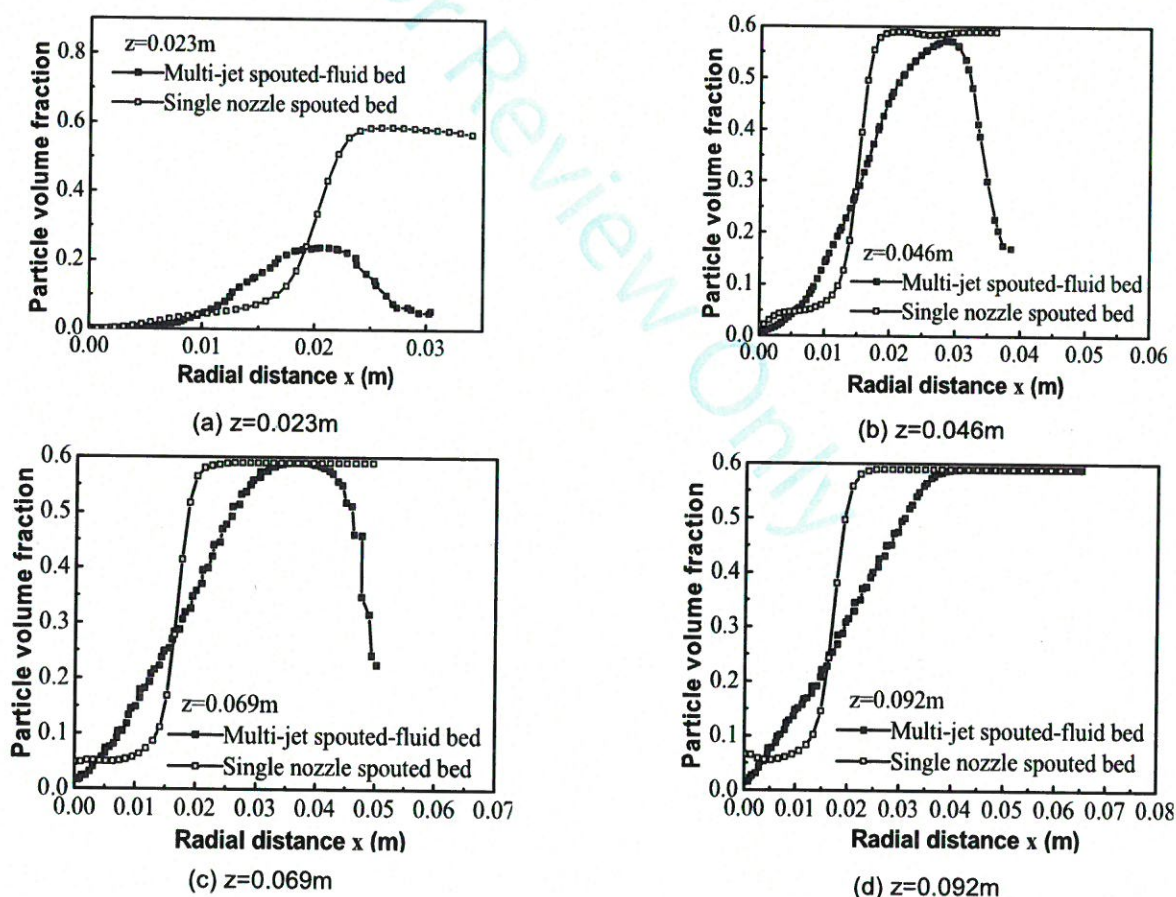


Fig.6 Comparison of concentration of particles in two kinds of spouted beds

3.2 Effect of integral multi-jet on flow of gas and particle phases

Figure 7 compares velocity and vorticity distribution of gas and particle phases in two kinds of spouted beds. It can be observed from Figure 7 (a) and Figure 7 (b) that, compared with the simulation results of single nozzle spouted bed, the range of the high speed region of gas and particle phases is significantly enlarged by auxiliary air jets in the IMJSFB, thus, the mutual penetration ability between gas and particle phases can be enhanced. As can be observed from Figure 7 (c), the vorticity distribution of gas phase also can be intensified by auxiliary air jets in spouted bed, at the same time, the influence range of vorticity is also extended effectively by gas fluidization in the cone side zone of spouted bed.

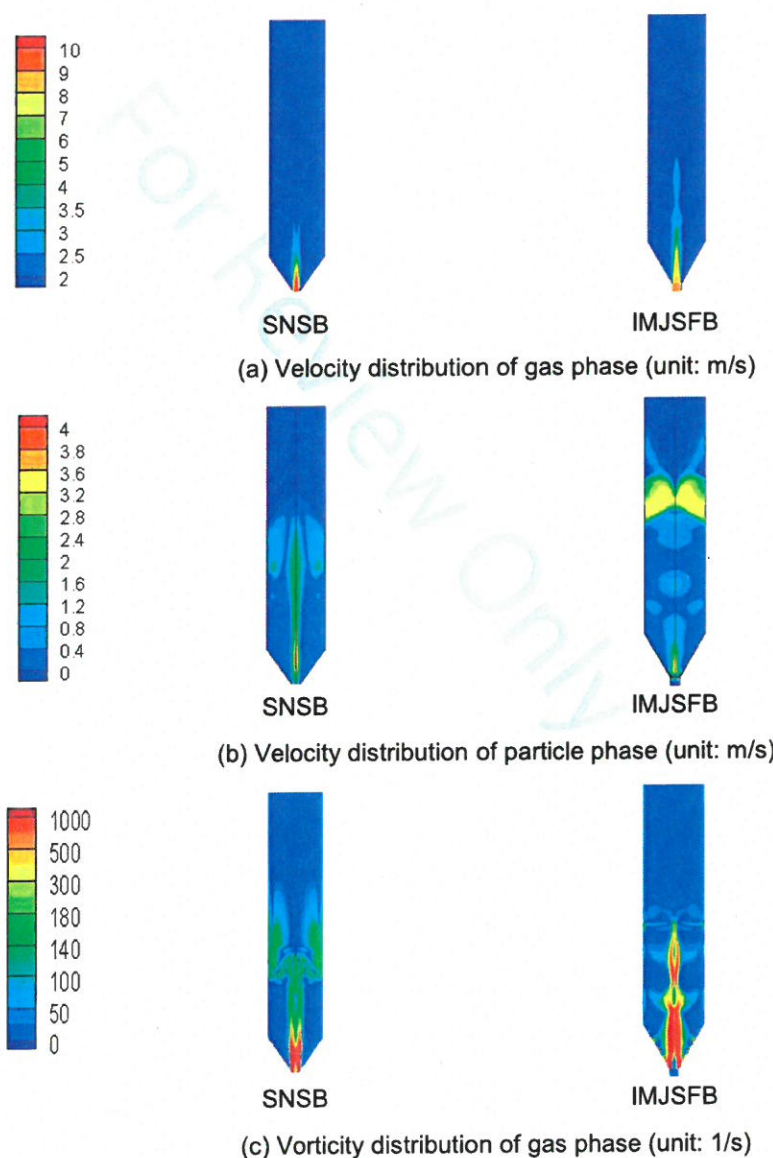


Fig.7 Comparison of velocity and vorticity distribution of gas and particle phases in two kinds of spouted beds

Figure 8 illustrates the comparison of particle velocity vector diagram in two kinds of spouted beds. It can be obviously seen that, compared with the velocity vector distribution in single nozzle spouted bed, a great deal of vortex flow of particle phase are formed on both sides of the axis in spouted bed due to the comprehensive movement effect of spout gas flow in the axial direction and the fluidizing gas flow from conical side of the IMJSFB, which indicates that the fluidizing gas can enhance diffusion and intensify particle mixing in the spouted bed, thus, the "dead zone" of particles in the conical section of the conventional cylindrical spouted bed can be eliminated.

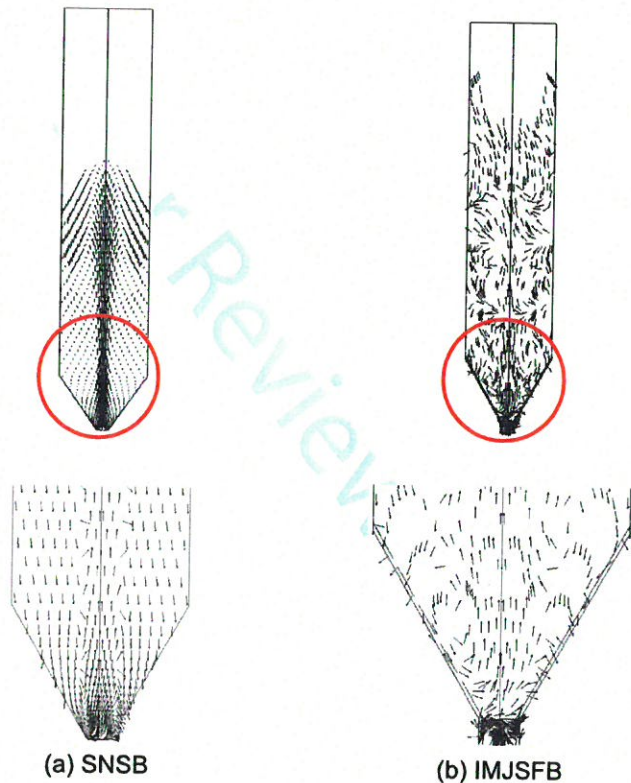


Fig.8 Comparison of particle velocity vector diagram in two kinds of spouted beds

Figure 9 shows the comparison of particle velocity along the radial direction in two kinds of spouted beds. It can be observed that the particle velocity in spout of the IMJSFB is much lower than that of conventional spouted bed, but particle velocity in the annulus is higher than that of conventional spouted bed. Also, the particle volume fraction in the IMJSFB presents a more uniform distribution along the radial direction, which reveals that, compared with the single nozzle spouted bed, the gas velocity in spout of the IMJSFB decreases because a part of the gas flows into the side jets as fluidizing gas, while the fluidizing gas strengthens the particle radial movement and increases the velocity of the particles in the annulus. The increase of particle velocity decreases with the increase of bed height as far away from the

1
2 fluidization zone of spouted bed.
3
4

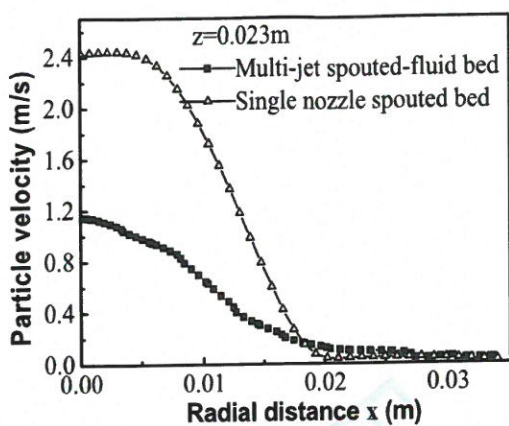
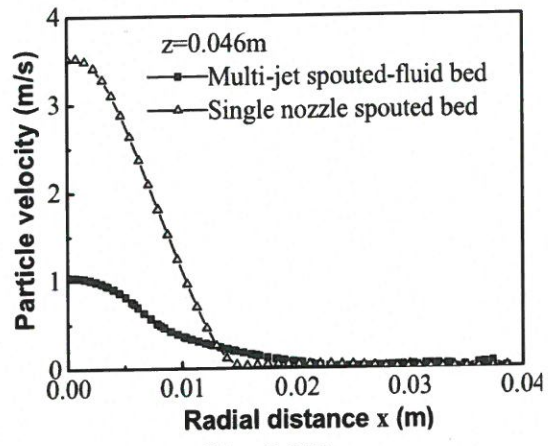
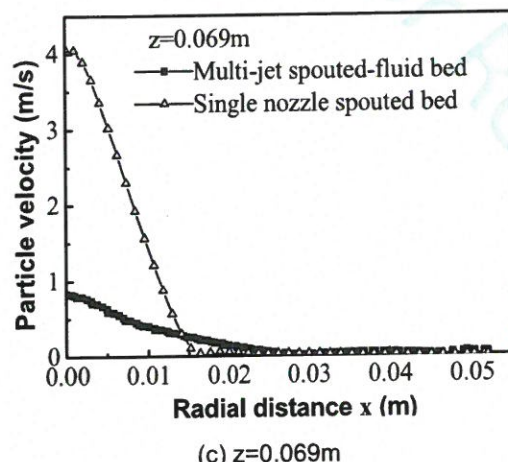
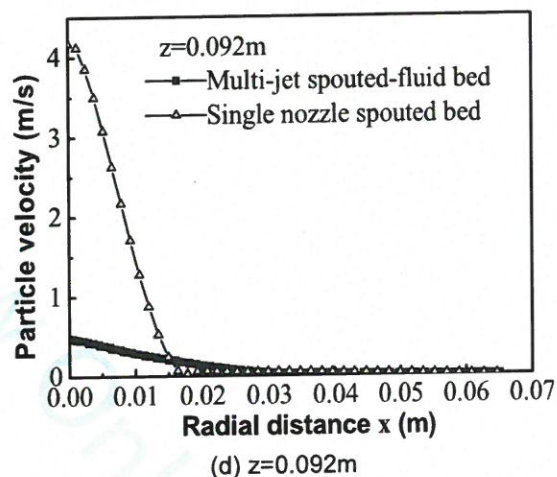
(a) $z=0.023\text{m}$ (b) $z=0.046\text{m}$ (c) $z=0.069\text{m}$ (d) $z=0.092\text{m}$

Fig.9 Comparison of particle velocity along radial direction in two kinds of spouted beds

In order to quantify the fluidization quality in spouted bed, the coefficient of variation (CV) of particles' velocity is adopted in this paper to analyze the flow field's uniformity, which is shown as follows:

$$CV = \left(S / \bar{V} \right) \times 100\% \quad (1)$$

$$S = \sqrt{\frac{1}{n-1} \sum_{j=1}^n (V_j - \bar{V})^2} \quad (2)$$

where S is the standard deviation, V_j is the velocity value of the sampling point, \bar{V} is the average velocity of all sample points, n is the number of samples. The uniformity of the flow field of particles in spouted bed is evaluated by comparing the CV values under different working conditions. Figure 10 illustrates comparison of CV of particles' velocity in two kinds of spouted beds. It can be observed that, compared with the single nozzle spouted bed (SNSB), the integral

multi-jet structure in spouted bed can significantly reduces the value of CV of particles' velocity in spouted beds, and the decrease in value of CV is 22.9% in the IMJSFB.

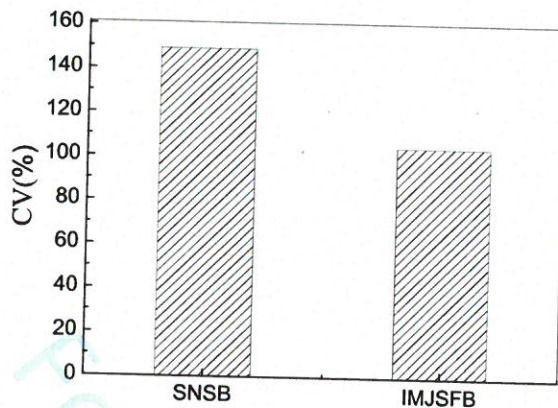


Fig.10 Comparison of CV of particles' velocity in two kinds of spouted beds

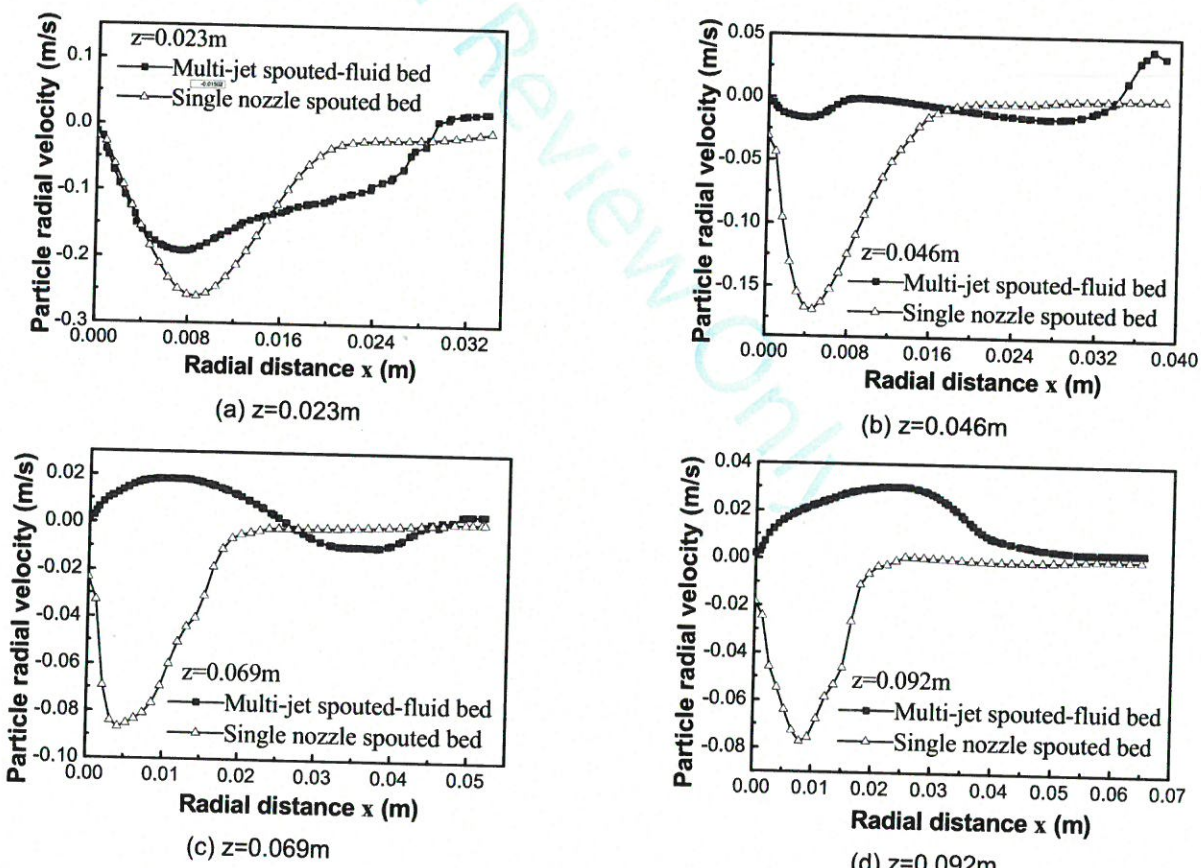


Fig.11 Comparison of particle radial velocity along radial direction in two kinds of spouted beds

Figure 11 displays comparison of particle radial velocity along radial direction in two kinds of spouted beds. It can be seen that, compared with the single nozzle spouted bed, the radial velocity distribution curve of the particles becomes more and more smooth along the radial direction in the IMJSFB. Especially, the radial velocity of particles in the annular gap is effectively improved by the fluidizing gas. The strengthening effect on particle radial velocity keeps good with the increase of the bed height due to the effective transverse permeability of gas in annulus of spouted bed.

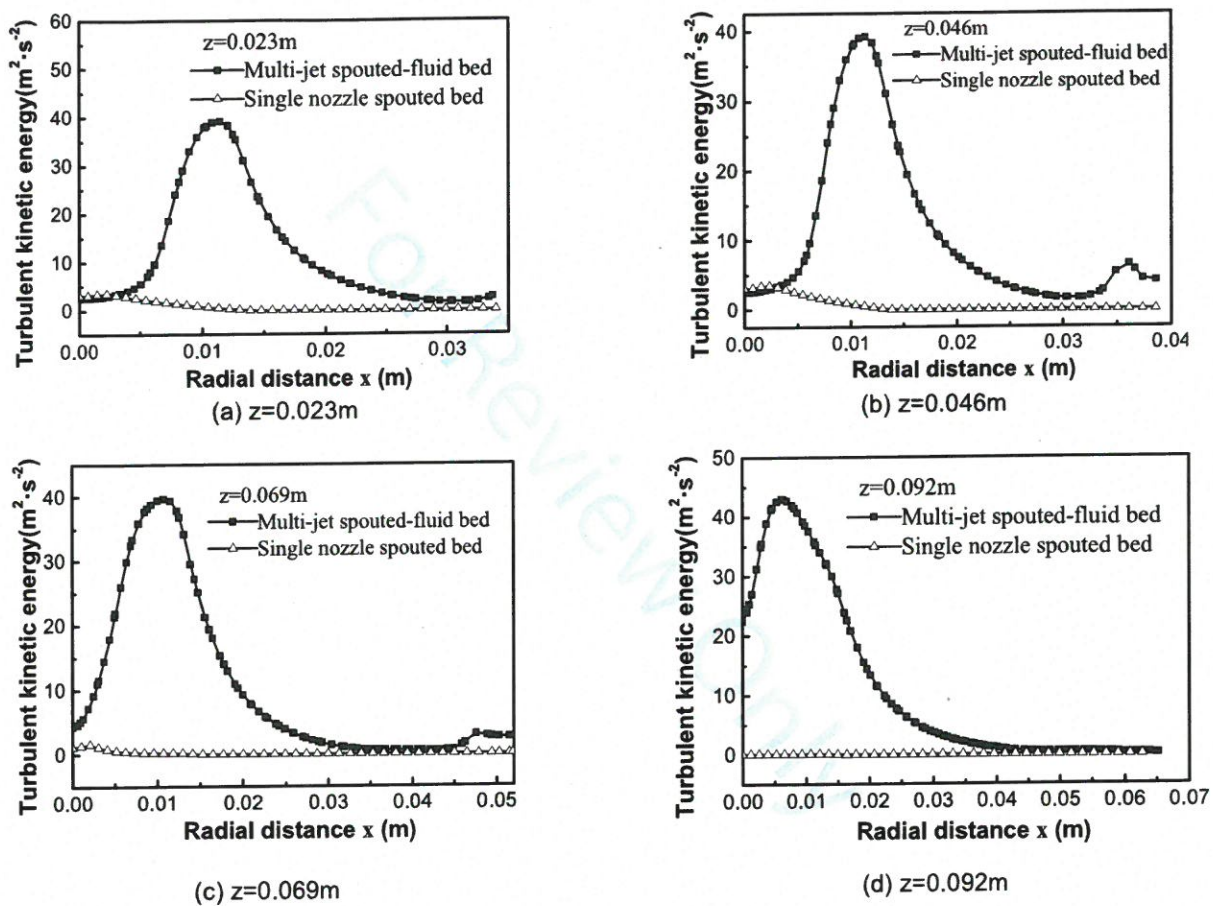


Fig.12 Comparison of turbulent kinetic energy of gas phase along radial direction in two kinds of spouted beds

In order to further study the fluidization effect of gas phase in spouted bed, the comparison of turbulent kinetic energy of gas phase along the radial direction in two kinds of spouted beds is showed in Figure 12. It can be observed that, compared with the single nozzle spouted bed, the fluidizing gas has significant impact on the turbulent kinetic energy of gas phase under the influence of the airflow in the spout zone, especially in the spout zone and near the annulus region, the turbulent kinetic energy of gas phase can be significantly enhanced by fluidizing gas and the strengthening effect on turbulent kinetic energy of gas keeps good with the increase of the bed height, which is

1
2
3 beneficial to strengthen radial mixing of gas and particle phases in the spout-fluidized bed. The IMJSFB has excellent
4 effect on particle' fluidization and the bypass fluidizing air supply auxiliary equipment can be omitted.
5
6
7
8 **4. Conclusions**
9
10

11 In this work, the gas-solid two phase flow characteristics in a novel IMJSFB was numerically studied by a two-fluid
12 model and the main conclusions of the present analysis are presented as follows:
13

14 (1) Compared with the solid volume fractions in single nozzle spouted bed, a wave like spout structure has been
15 formed in the IMJSFB because the additional bubbles emerges caused by fluidizing gas and enter the spout zone and
16 the area of spout region becomes wider in spouted bed.
17
18

19 (2) The fluidizing gas can effectively reduce the particle' volume fraction in the annulus zone, the particle volume
20 fraction along the radial distribution becomes more uniform, which is beneficial to eliminate the "dead zone" of particle
21 flow at the cone, thus improving the motion state of the particles and the gas-solid contact efficiency in the annular
22 region, especially in the near cone region.
23
24

25 (3) Compared with the velocity vector distribution in the SNSB, a great deal of vortex flow of particle phase are
26 formed on both sides of the axis in the IMJSFB, thus, the "dead zone" of particles in the conical section of the
27 conventional cylindrical spouted bed can be eliminated. Also, the decrease in value of CV of particles' velocity is 22.9%
28 in the IMJSFB.
29
30

31 (4) The turbulent kinetic energy of gas phase can be significantly enhanced by fluidizing gas and the strengthening
32 effect on turbulent kinetic energy of gas keeps good with the increase of the bed height. The IMJSFB has excellent
33 effect on particle' fluidization and the bypass air supply auxiliary equipment can be omitted.
34
35

45 **ACKNOWLEDGEMENT**

46 This work is supported by National Natural Science Foundation of China (Grant No. 21476181), China Postdoctoral
47 Science special Foundation (Grant No. 2015T81048), China Postdoctoral Science Foundation funded project (Grant No.
48 2013M540768) and Cyrus Tang Foundation.
49
50
51
52
53
54
55
56
57
58
59
60

References

- Epstein, N., Grace, J. R., Spouted and spout-fluid beds: fundamental and applications. Cambridge University Press, 2011.
- Ichikawa, H., Arimoto, M., Fukumori, Y., Design of microcapsules with hydrogel as a membrane component and their preparation by spouted bed. *Powder Technology*, 130, 189–192 (2003).
- Freitas, L.A.P., Freire, J.T., Experimental study on the dynamics of a spouted bed with particle feed through the base. *Brazilian Journal of Chemical Engineering*, 14, 269–280 (1997).
- Olazar, M., Aguado, R., Sánchez, J.L., Bilbao, R., Arauzo, J., Thermal processing of straw black liquor in fluidized and spouted bed. *Energy & Fuels*, 16, 1417–1424 (2002).
- Niksiar, A., Sohrabi, M., A novel hydrodynamic model for conical spouted beds based on stream tube modeling approach. *Powder Technology*, 267, 371 – 380 (2014).
- Xavier, T.P., Libardi, B.P., Lira, T. S., Barrozo, M. A.S., Fluid dynamic analysis for pyrolysis of macadamia shell in a conical spouted bed. *Powder Technology*, 299, 210 – 216 (2016).
- Parise, M. R., Wang, Z., Lim, C.J., Grace, J.R., Hydrodynamics of a slot-rectangular spouted bed of biomass particles with simultaneous injection of spouting and pulsating air streams. *Chemical Engineering Journal*, 330, 82 – 91 (2017).
- Kiani, M., Rahimi, M.R., Hosseini, S.H., Ahmadi, G., Mixing and segregation of solid particles in a conical spouted bed: Effect of particle size and density. *Particuology*, 32, 132 – 140 (2017).
- Szafran, R.G., Kmiec, A., CFD modeling of heat and mass transfer in a spouted bed dryer. *Industrial and Engineering Chemistry Research*, 43, 1113–1124 (2004).
- Liu, M., Liu, B., Shao, Y. L., Optimization of the UO₂ kernel coating process by 2D simulation of spouted bed dynamics in the coater. *Nuclear Engineering and Design*, 251, 124–130 (2012).
- Hosseini, S. H.;Fattah, M.; Ahmadi, G. Investigation of hydrodynamics and heat transfer in pseudo 2D spouted beds with and without draft plates. *Brazilian Journal of Chemical Engineering*, 34(4), 997-1009 (2017).
- Wu, F., Gao, W., Zhang, J., Ma, X., Zhou, W., Numerical analysis of gas-solid flow in a novel spouted bed structure under the longitudinal vortex effects. *Chemical Engineering Journal*, 334, 2105-2114 (2018).
- Sutanto, W., Epstein, N., Grace, J. R., Hydrodynamics of spout-fluid beds. *Powder Technology*, 44, 205–212 (1985).
- Zhao, J., Lim, C. J., Grace, J. R., Flow regimes and combustion behavior in coal-burning spouted and spouted-fluid beds. *Chemical Engineering Science*, 42, 2865–2875 (1987).
- St. M., Apnold, J., Gale, J. J., Laughlin, M. K., The British coal spouted fluidized bed gasification process. *The Canadian Journal of Chemical Engineering*, 70(5), 991-997 (1992).
- Pianarosa, D. L., Freitas, L. A. P., Lim, C. J., Grace, J. R., Dogan, O. M., Voidage and particle velocity profiles in a spout-fluid bed. *The Canadian Journal of Chemical Engineering*, 78, 132–142 (2000).
- Zhong, W., Zhang, M., Characterization of dynamic behavior of a spout-fluid bed with Shannon entropy analysis. *Powder Technology*, 159, 121–126 (2005).
- [19] Zhong, W., Zhang, M., Jet penetration depth in a two-dimensional spout-fluid bed. *Chemical Engineering Science*, 60, 315–327 (2005a).
- Zhong, W., Zhang, M., Pressure fluctuation frequency characteristics in a spout-fluid bed by modern ARM power spectrum analysis. *Powder Technology*, 152, 52–61 (2005b).
- Wang, S., Zhao, L., Wang, C., Liu, Y., Gao, J., Liu, Y., Cheng, Q., Numerical simulation of gas–solid flow with two fluid model in a spouted-fluid bed. *Particuology*, 14, 109–116 (2014).
- Nagashima, H., Kawashiri, Y., Suzukawa, K., Ishikura, T., Effects of operating parameters on hydrodynamic behavior of spout-fluid beds without and with a draft tube. *Procedia Engineering*, 102, 952–958 (2015).
- Sutkar, V. S., Deen, N. G., Patil, A. V., Salikov, V., Antonyuk, S., Heinrich, S., Kuipers, J.A.M., CFD - DEM model for

- 1
2
3 coupled heat and mass transfer in a spout fluidized bed with liquid injection. Chemical Engineering Journal, 288,
4 185–197 (2016).
5
6 Monazam, E. R., Breault, R. W., Weber, J., Analysis of maximum pressure drop for a flat-base spouted fluid bed.
7 Chemical Engineering Research and Design, 122, 43–51 (2017).
8
9 Monazam, E. R., Breaulta, R. W., Webera, J., Layfield, K., Minimum spouting velocity of flat-base spouted fluid bed.
10
11 Gidaspow, D., Bezburuah, R., Ding, J., Hydrodynamics of circulating fluidized beds. Kinetic Theory Approach,
12 Fluidization VII. In: Proceedings of the Seventh Engineering Foundation Conference on Fluidization, 75-82,
13 (1992a).
14
15 Ding, J., Gidaspow, D., A bubbling fluidization model using kinetic theory of granular flow. Aiche Journal, 36, 523-538
16
17 Lun, C.K., Savage, S.B., Jeffrey, D.J., Chepurniy, N., Kinetic theories for granular flow: inelastic particles in Couette flow
18 and slightly inelastic particles in general flow field. Journal of Fluid Mechanics, 140, 223-256 (1984).
19
20 Schaeffer, D.G., Instability in the evolution equations describing incompressible granular flow. Journal of Differential
21 Equations, 66, 19-50 (1987).
22
23 Du, W., Xu, X., Xu, J., Wei, W., Computational fluid dynamics (CFD) modeling of spouted bed: influence of frictional
24 stress, maximum packing limit and coefficient of restitution of particles. Chemical Engineering Science, 61,
25 4558-4570 (2006).
26
27 Lauder, B.E., Sharma, B.I., Application of the energy-dissipation model of turbulence to the calculation of flow near a
28 spinning disc. Lett. Heat Mass transfer, 1, 131-138 (1974).
29
30 Yakhot, V., Orzag, S.A., Renormalization group analysis of turbulence: basic theory. J Scient Comput, 1. 3-11 (1986).
31
32 Shih, T.H., Liou, W.W., Shabbir, A., Yang, Z.G., Zhu, J., A new $k-\epsilon$ eddy viscosity model for high Reynolds number
33 turbulent flows. Comput Fluids, 24(3), 227-238 (1995).
34
35 He, Y.L., Lim, C.J., Grace, J.R., Zhu, J., Qzn, S., Measurements of voidage profiles in spouted beds. Canadian Journal
36
37 of Chemical Engineering, 72, 229-234 (1994).
38
39 Y.L. He, S.Z. Qin, C.J. Lim, Grace, J.R., Particle velocity profiles and solid flow patterns in spouted beds. Canadian
40
41 Journal of Chemical Engineering, 72, 561-568 (1994a).
42
43
44
45
46
47
48
49
50
51
52
53
54
55
56
57
58
59
60

1
2
3 **NOMENCLATURE**

| | | |
|----------------------|-------------------------------|--|
| C_D | [—] | Drag coefficient, dimensionless |
| CV | [—] | Coefficient of variation |
| d_s | [mm] | Particle diameter |
| D_i | [mm] | Diameter of the spouted gas inlet |
| D | [mm] | Diameter of the bed |
| e_s | [—] | Coefficient of restitution of particle |
| g_0 | [—] | Radial distribution coefficient |
| H | [mm] | Vessel height |
| H_0 | [mm] | Static bed depth |
| k | [m^2/s^2] | Turbulent kinetic energy |
| I | [—] | Stress tensor |
| P | [—] | Pressure |
| P_s | [—] | Solid pressure |
| Re | [—] | Reynolds number |
| t | [s] | Time |
| U | [m/s] | Superficial gas velocity |
| U_{ms} | [m/s] | Minimum spouting velocity |
| x, z | [m] | Cartesian coordinates |
| <i>Greek symbols</i> | | |
| α_g | [—] | Gas volume fraction |
| α_s | [—] | Solids volume fraction |
| β_{gs} | [kg/(m^3s)] | Fluid-particle friction coefficient |
| θ | [m^2/s^2] | Granular temperature |
| γ_s | [kg/(m^3s)] | Energy dissipation |
| μ_g | [Pas] | Gas viscosity |
| μ_s | [Pas] | Particle viscosity |
| ρ | [kg/ m^3] | Density |
| μ | [kg/(ms)] | Shear viscosity |
| τ | [Pa] | Stress tensor |
| ϕ | [deg] | Angle of internal friction |
| ε | [m^2/s^3] | Turbulence dissipation of gas phase |
| <i>subscripts</i> | | |
| g | [—] | Gas |
| q | [—] | Phase type(solid or gas) |
| s | [—] | Solids |

